ACS OMEGA

Open Access

http://pubs.acs.org/journal/acsodf

Article

Synthesis and Anticancer Activity Evaluation of Novel Carborane-Containing Isoflavonoid Analogues

Yirong Zhang,† Chuwei Yu,† Linyuan Wang, Lina Zhou, Chaofan Li, Changxian Yuan, Nan Sun, Guanxiang Hao, Chenyang Ma, Yuzhe Lin, Hongjing Li, Jiali Hong, Jinhua Zhao, Kaiyan Lou, Rui Zhang,* Chengying Xie,* and Sinan Wang*

Cite This: *ACS Omega* 2025, 10, 18720−18732

Read Online

ACCESS | Metrics & More | Article Recommendations | Supporting Information

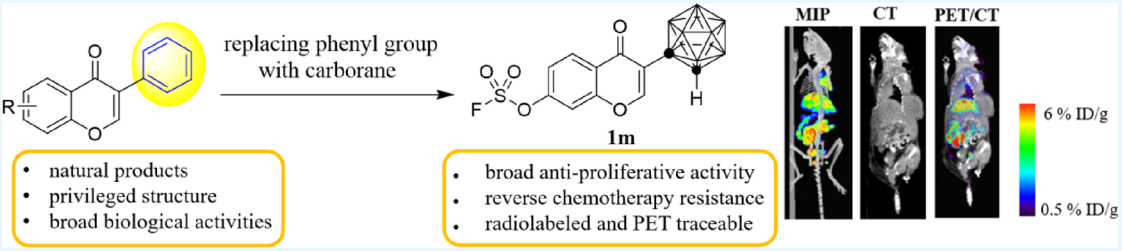

ABSTRACT: Isoflavonoids represent a privileged structure derived from natural products with diverse bioactivities. Carborane has been utilized as a three-dimensional mimetic of phenyl rings in medicinal chemistry. Herein, we replaced the phenyl group of isoflavonoids with carborane and prepared a series of carborane-containing isoflavonoid analogues. Compounds **1d**, **1g**, and **1m** showed significantly enhanced antiproliferative activities on a broad scope of cancer cell lines. Further studies indicated that both **1d** and **1m** inhibited JAK/STAT5, PI3K/AKT, and p38 MAPK pathways, leading to G1 cell cycle phase arrest. Additionally, both compounds reduced the expression of P-glycoprotein (P-gp), a key mediator in multidrug resistance, and reversed the resistance of chemotherapeutic agents in multidrug-resistant cells *in vitro*. The biodistribution of compounds **1d** and **1m** was evaluated through ICP-mass and positron emission tomography imaging studies. Taken together, these results suggested promising pharmaceutical properties for the carborane-containing isoflavonoid analogues.

INTRODUCTION

Natural products and their derivatives have been explored as invaluable sources for medicinal chemistry and drug discovery.[1,2] Modification of natural products represents an effective strategy for improving their potency and druglike properties.[3,4] Isoflavonoids belong to a subclass of the natural product flavonoids primarily present in food, such as soybeans. It is structurally characterized by a 3-phenylchroman scaffold, which is considered as a privileged structure in medicinal chemistry.[5,6] Isoflavonoids exhibited broad biological activities including estrogenic activity, antitumor, anti-inflammatory, antioxidant, and neuroprotective effects.[7−10] Isoflavonoid compounds such as genistein and daidzein are considered as both preventive and therapeutic agents for cancer, particularly for breast and prostate cancer (Figure 1).[11,12]

In recent years, the application of carborane as a pharmacophore has regained attention.[13,14] Carborane are boron clusters containing 10 BH and 2 CH vertices with the molecular formula $C_2B_{10}H_{12}$. The high boron content makes it an ideal boron agent for boron neutron capture therapy (BNCT).[15] In addition, it also exhibits unique physical and chemical properties including high stability *in vivo*, high hydrophobicity, comparable volume to a rotational phenyl ring, and unusual dihydrogen bonds.[16] Given the similar properties between carborane and a phenyl group, carborane has been utilized as a three-dimensional mimetic of phenyl rings in medicinal chemistry. So far, several studies have used this strategy to modify drugs such as aspirin, flurbiprofen, or estrogen inhibitors.[17−20] However, incorporating carborane into natural products is rarely reported.[21]

Positron emission tomography (PET) is a noninvasive medical imaging technique that can visualize radiolabeled molecules *in vivo* at a high sensitivity.[22,23] It has been widely used in nuclear medicine and is increasingly applied for drug discovery.[24−26] PET imaging of radiolabeled natural product analogues can facilitate our understanding of their *in vivo* properties including pharmacokinetics, biodistribution, target accumulation, and effective dosing.[27]

Received: January 9, 2025
Revised: March 5, 2025
Accepted: March 12, 2025
Published: April 29, 2025

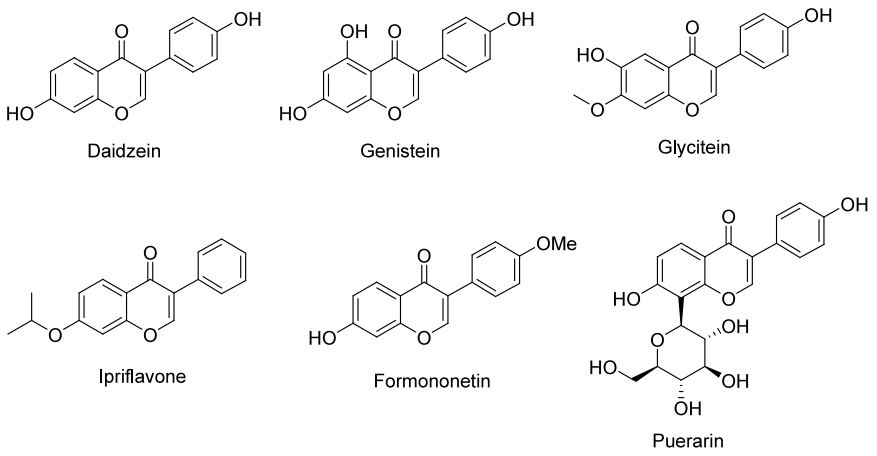

Figure 1. Structures of representative bioactive compounds with isoflavonoid scaffolds.

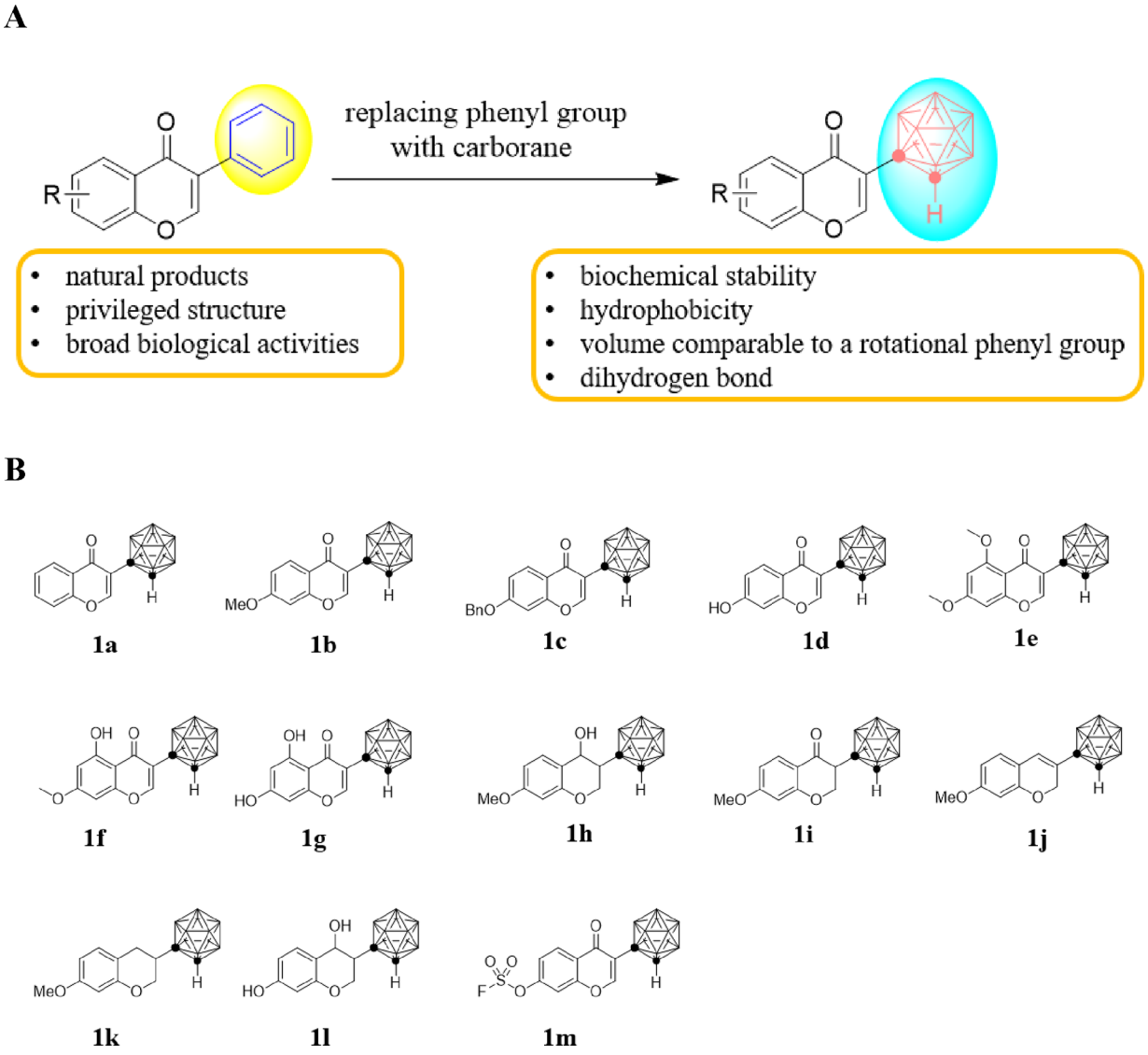

Figure 2. (A) Design of carborane-containing isoflavone derivatives. (B) Structures of carborane-containing isoflavone derivatives in this study.

Since the isoflavonoids represent a privileged structure derived from natural products with broad biological activities and contain a phenyl ring in its scaffold, we hypothesize that replacing the phenyl ring with carborane could provide unique properties to the biological activities of isoflavonoids. Herein, we report the synthesis and biological evaluation for a series of carborane-containing isoflavonoid compounds. In addition, compound **1m** was radiolabeled with ^{18}F using a SuFEx

https://doi.org/10.1021/acsomega.5c00262
ACS Omega 2025, 10, 18720−18732

Scheme 1. Synthesis of Compounds 1a−1g[a]

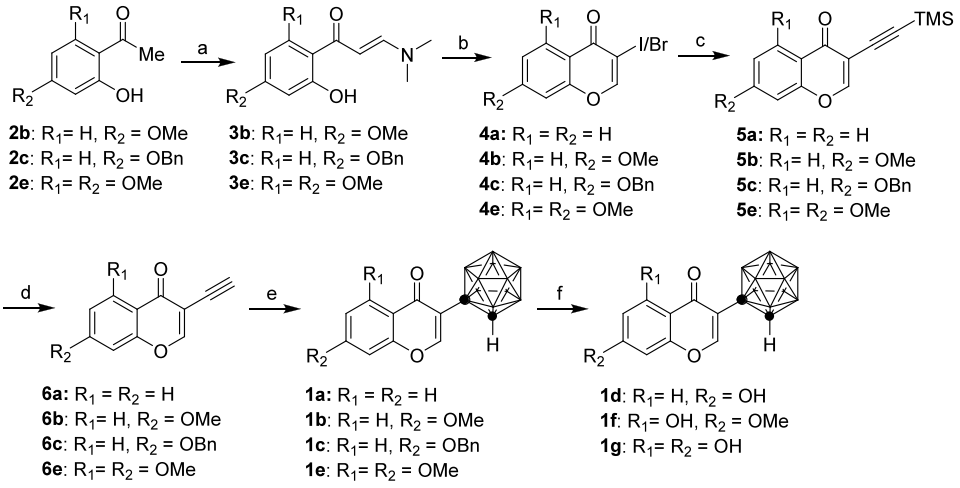

[a]Reagents and conditions: (a) *N,N*-dimethylformamide dimethyl acetal, DMF, 70 °C (b); I_2, MeOH, 40 °C; (c) trimethylsilylacetylene, $Pd(PPh_3)_2Cl_2$, CuI, Et_3N, rt; (d) CSA, TBAF, THF, rt; (e) $B_{10}H_{12}(CH_3CN)_2$, (Bmim)Cl, PhMe, 110 °C; (f) BBr_3, DCE, 40 °C or 70 °C.

Scheme 2. Synthesis of Compounds 1h−1k[a]

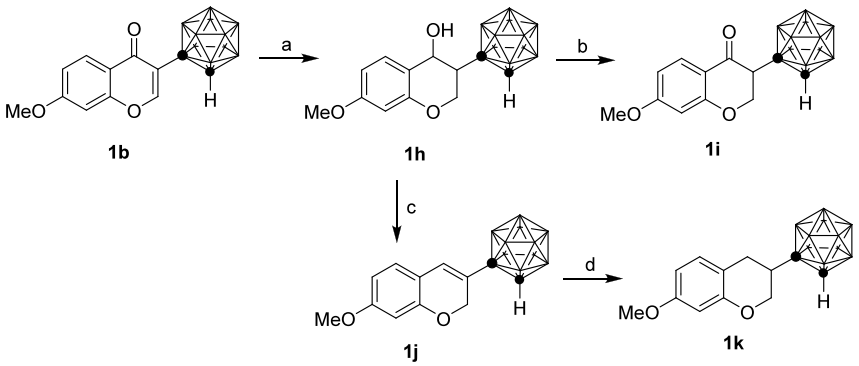

[a]Reagents and conditions: (a) $NaBH_4$, THF, rt; (b) MnO_2, DCM, rt; (c) polyphosphoric acid, DCE, reflux; (d) H_2, Pd/C, THF, rt.

reaction followed by a PET imaging study to demonstrate its biodistribution in tumor-bearing mice.

RESULTS AND DISCUSSION

Compound Design. Isoflavonoids contain a phenyl group attached to the chroman scaffold. In order to discover novel isoflavonoid analogues with improved biological activities, we replaced the phenyl group in isoflavonoid with *o*-carborane (Figure 2A). A series of novel carborane-containing isoflavones with various substitutions on the chromone core were prepared (compounds **1a−1g**). Furthermore, this scaffold was modified by a reducing, oxidizing, or eliminating reaction to produce a series of carborane-containing isoflavonoid derivatives (compounds **1h−1l**). Finally, compound **1m** was synthesized by introducing the fluorosulfate group to the scaffold for PET imaging studies (Figure 2B).

Chemistry. The synthesis of compounds **1a−1g** is shown in Scheme 1. Starting materials **2b**, **2c**, **2e**, and **4a** are commercially available. Briefly, compounds **2b**, **2c**, or **2e** were reacted with *N,N*-dimethylformamide dimethyl acetal to form compound **3**. Iodine was added to trigger a cyclization reaction to form compound **4**. Sonogashira coupling of compound **4** with trimethylsilyl acetylene followed by a deprotection formed compound **6**. Reacting compound **6** with $B_{10}H_{12}(MeCN)_2$ produced our target compounds **1a**, **1b**, **1c**, and **1e**. Compounds **1b** and **1e** were reacted with BBr_3 at different temperatures to remove the methyl group and yielded final products **1d**, **1f**, and **1g**.

The synthesis of compounds **1h−1k** is shown in Scheme 2. We found that reacting compound **1b** with $NaBH_4$ resulted in the reduction of both the ketone group and the alkene group to generate compound **1h**. Oxidizing compound **1h** with MnO_2 produced compound **1i**. Heating compound **1h** with polyphosphoric acid generated the elimination product compound **1j**. Reducing compound **1j** in a hydrogen atmosphere yielded compound **1k**.

The synthesis of compounds **1l** and **1m** is shown in Scheme 3. Mixing compound **1d** with $NaBH_4$ reduced both the ketone group and the alkene group to generate compound **1l**. Compound **1d** was reacted with 1-(fluorosulfonyl)-2,3-dimethyl-1*H*-imidazol-3-ium to yield compound **1m**.

Biological Evaluation. *Antiproliferative Activities of Carborane-Containing Isoflavonoid Derivatives against Tumor Cell Lines.* The human breast cancer cell line MDA-MB-231 and human prostate cancer cell line PC-3 were used to determine the activities of isoflavonoid derivatives on tumor cell proliferation.[28] The IC_{50} values of the tested compounds are shown in Table 1. Compound **1a** represents the scaffold of the carborane-containing isoflavone and showed weak antiproliferative activities with IC_{50} greater than 50 μM.

https://doi.org/10.1021/acsomega.5c00262
ACS Omega 2025, 10, 18720−18732

Scheme 3. Synthesis of Compounds 1l and 1m[a]

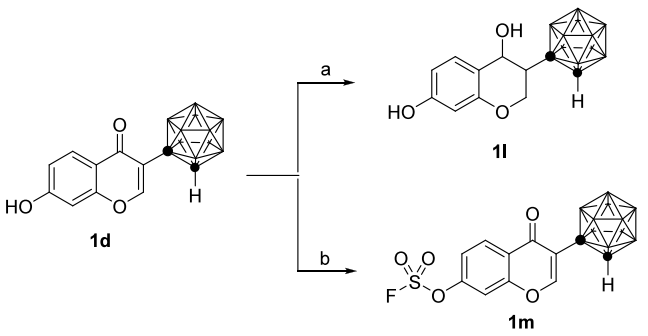

[a]Reagents and conditions: (a) $NaBH_4$, THF, rt; (b) 1-(fluorosulfonyl)-2,3-dimethyl-1*H*-imidazol-3-ium trifluoromethanesulfonate, Et_3N, MeCN, rt.

Table 1. *In Vitro* Antiproliferative Activities of Carborane-Containing Isoflavonoid Derivatives[a]

	IC$_{50}$ (μM)	
compounds	MDA-MB-231	PC-3
1a	75.17 ± 20.80	66.58 ± 8.79
1b	47.54 ± 7.39	54.71 ± 6.26
1c	65.29 ± 5.39	72.40 ± 1.06
1d	5.59 ± 1.82	5.24 ± 1.90
1e	55.79 ± 6.71	53.09 ± 0.73
1f	>100	>100
1g	5.34 ± 1.03	5.14 ± 2.93
1h	14.63 ± 1.58	13.45 ± 1.02
1i	25.42 ± 7.30	38.02 ± 2.79
1j	15.96 ± 0.16	10.86 ± 3.31
1k	35.34 ± 4.78	35.51 ± 0.98
1l	17.93 ± 6.09	16.61 ± 1.89
1m	5.46 ± 0.61	4.99 ± 2.76
formononetin	>100	>100
genistein	36.93 ± 2.81	29.53 ± 8.74

[a]Data were expressed as means ± SD ($n \geq 2$).

Compounds **1b** and **1c** with methoxy or benzyloxy groups on the chromone moiety also showed minimal activities. To our delight, compound **1d** exhibited significantly increased activity (5.59 μM for MDA-MB-231 and 5.24 μM for PC-3), suggesting the importance of the phenolic hydroxyl group. The dimethoxyl-substituted compound **1e** also showed little activity against these two cell lines. Interestingly, compound **1f** with a hydroxyl group on the 5 position and a methoxyl group on the 7 position exhibited no activity, while compound **1g** with a 5,7-dihydroxyl group displayed much improved antitumor activity (5.34 μM for MDA-MB-231 and 5.14 μM for PC-3). These results again suggested that the phenolic hydroxyl group on the 7 position of the carborane-containing isoflavone is a key pharmacophore for its antiproliferative activity. The reduced compounds **1h** and **1i** with a methoxy group on the 7 position showed moderate inhibition activities (14.63 and 25.42 μM for MDA-MB-231 and 13.45 and 38.02 μM for PC-3). Compounds **1j** and **1k** with the removal of the ketone group showed similar activities compared to **1h** and **1i**. The reduced compound **1l** with a hydroxy group on the 7 position also exhibited an improved inhibition activity (17.93 μM for MDA-MB-231 and 16.61 μM for PC-3). To our surprise, compound **1m** with a fluorosulfate group at position 7 displayed the most potent activity (5.46 μM for MDA-MB-231 and 4.99 μM for PC-3). As a comparison, two bioactive isoflavone compounds were selected to test their antiproliferative activities. Formononetin exhibited no activity, and genistein displayed a moderate antiproliferative effect. These results demonstrated that in this case, replacing the phenyl ring with carborane is an effective strategy to improve the antiproliferative activities of isoflavonoid compounds.

Since compounds **1d**, **1g**, and **1m** are the most potent among these compounds, they were selected to test their antiproliferative activities on a large scale of cancer cell lines derived from different tissues, including solid tumors and hematologic malignancies. These three compounds exhibited antiproliferative activities toward all the tested 13 cancer cell lines with the IC$_{50}$ values ranging from 1.93 to 7.00 μM (Table 2), suggesting a broad anticancer spectrum for these compounds. Although these three compounds exhibited varying cytotoxic effects against different cell lines, no significant tissue specificity was observed.

*Compounds **1d** and **1m** Induce G1 Cell Cycle Phase Arrest.* To reveal the mechanism by which carborane-containing isoflavonoid derivatives inhibit cancer cell proliferation, we initially examined their effect on the cell cycle using flow cytometry. The majority of the studies in this field

Table 2. Antiproliferative Activities of Selected Compounds in Various Cultured Cell Lines[a]

		IC$_{50}$ (μM)		
tissue origin	cell line	**1d**	**1g**	**1m**
breast carcinoma	MDA-MB-231	5.59 ± 1.82	5.34 ± 1.03	5.46 ± 0.61
prostate carcinoma	PC-3	5.24 ± 1.90	5.14 ± 2.93	4.99 ± 2.76
lung carcinoma	H1975	5.27 ± 0.63	5.13 ± 1.08	5.63 ± 0.30
	NCI-H460	4.24 ± 0.90	5.93 ± 2.15	3.19 ± 0.18
squamous cell carcinoma	A-431	4.09 ± 0.46	4.84 ± 1.07	4.86 ± 0.21
pancreatic carcinoma	HPAF-II	3.56 ± 0.38	4.14 ± 0.93	2.67 ± 0.55
gastric carcinoma	NUGC-3	3.36 ± 0.02	4.79 ± 0.44	2.54 ± 0.37
	KATO III	4.38 ± 0.04	5.02 ± 0.38	3.55 ± 0.15
colorectal carcinoma	HCT116	3.42 ± 0.22	4.21 ± 0.11	2.86 ± 0.23
diffuse large B cell lymphoma	DOHH2	2.78 ± 0.26	5.23 ± 0.62	1.93 ± 0.12
	SUDHL-4	5.40 ± 0.48	6.16 ± 0.34	4.29 ± 0.54
chronic myeloid leukemia	K562	5.29 ± 0.86	7.00 ± 0.27	4.52 ± 0.80
acute myeloid leukemia	MV-4-11	4.25 ± 0.34	5.65 ± 0.02	5.45 ± 0.26

[a]Data were expressed as means ± SD ($n \geq 2$).

https://doi.org/10.1021/acsomega.5c00262
ACS Omega 2025, 10, 18720−18732

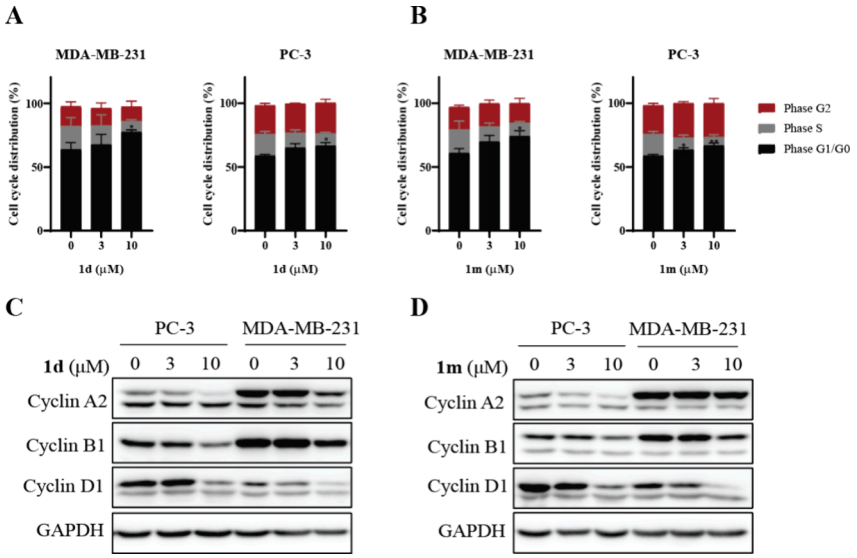

Figure 3. Compounds **1d** and **1m** induce G1 cell cycle phase arrest. MDA-MB-231 and PC-3 cells were treated with **1d** (A) or **1m** (B) for 24 h. The cell cycle distribution was analyzed by PI staining via flow cytometry. Numbers on the vertical coordinate indicated the proportion of cells in each phase of the cell cycle. Western blot analyses of cell cycle-related proteins in MDA-MB-231 and PC-3 cell lines after 24 h of treatment with a concentration gradient of **1d** (C) or **1m** (D) were shown. Data were presented as means ± SD. Statistical significance was assessed using a two-tailed unpaired Student's *t* test. $^{*}P < 0.05$, $^{**}P < 0.01$.

have demonstrated that treatment with formononetin induced sub-G0/G1 and G1 cell cycle arrest in cancer cells by modulating the expressions of cyclin regulatory proteins.[29] Accordingly, our data showed that **1d** (Figure 3A) and **1m** (Figure 3B) caused G0/G1 cell cycle arrest in both MDA-MB-231 and PC-3 cells. Furthermore, in this study, both **1d** and **1m** downregulated the expression of G0/G1 cell cycle-related proteins, such as cyclin A2, cyclin B1, and cyclin D1 in a dose-dependent manner (Figure 3C,D). Thus, the beneficial effects of isoflavonoid may be attributed to its antiproliferative and cell cycle arrest-inducing properties.

*Compounds **1d** and **1m** Inhibit JAK/STAT5, PI3K/AKT, and p38 MAPK Pathways.* Formononetin has been demonstrated to regulate various transcription factors and growth factor-mediated oncogenic pathways, thereby inducing cell cycle arrest and suppressing cell proliferation.[30] As shown in Figure 4, both **1d** and **1m** reduced the expression of P-AKT, P-STAT3, and P-STAT5 while upregulating P-P38 expression in MDA-MB-231 (Figure 4A) and PC-3 cells (Figure 4B) in a concentration-dependent manner. Collectively, these findings suggest that carborane-containing isoflavonoid derivatives exhibited antitumor activity through modulation of the JAK/STAT5, PI3K/AKT, and p38 MAPK pathways.

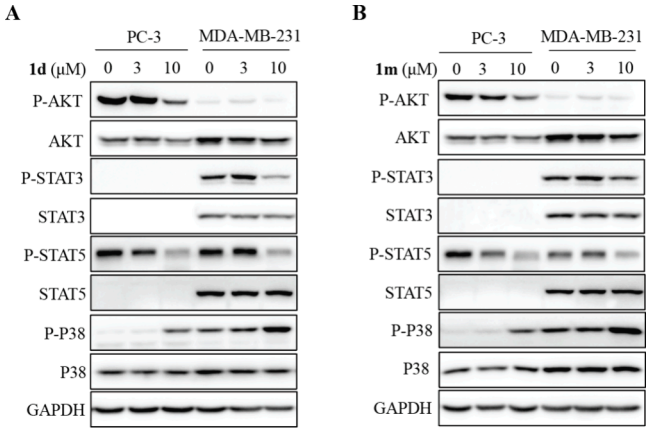

Figure 4. Compounds **1d** and **1m** inhibit the JAK/STAT5, PI3K/AKT, and p38 MAPK pathways. Western blot analyses of MDA-MB-231 and PC-3 cell lines after treatment with a concentration gradient of **1d** (A) or **1m** (B) for 24 h.

*Compounds **1d** and **1m** Maintain Their Potency in K562/ADR Cells and Enhance the Sensitivity of Cytotoxic Drugs by Downregulating MDR1.* The main challenge in cancer chemotherapy is multidrug resistance (MDR), driven by ATP-binding cassette transporters, with P-glycoprotein (P-gp) overexpression playing a crucial role. P-gp actively pumps chemotherapeutic agents out of tumor cells in an ATP-dependent mechanism, leading to reduced drug accumulation and ultimately chemotherapeutic failure.[31] To assess the potential of carborane-containing isoflavonoid derivatives in overcoming drug resistance, we investigated the impact of **1d** and **1m** on MDR cell subline K562/ADR. We utilized three conventional anticancer drugs—adriamycin (ADR), paclitaxel (PTX), and vinorelbine (VRN)—that are known to be expelled by P-gp.[32] Both **1d** and **1m** demonstrated significant cytotoxicity in K562/ADR compared with parental cell line K562. The average resistance factors (RFs) of **1d** and **1m** in K562/ADR cells were 0.93 and 0.67, respectively, in contrast to 230.86, 106.35, and over 6000 for VRN, ADR, and PTX, respectively (Table 3). These findings suggest reduced cytotoxicity in K562/ADR cells due to the efflux of cytotoxic drugs, confirming the P-gp phenotype of the cell line while also indicating maintained sensitivity to carborane-containing isoflavonoid derivatives.

To explore the antimultidrug resistance mechanism, we detected the expression of MDR1. Compared to K562, K562/ADR exhibited elevated expression of MDR1, which was significantly inhibited by both **1d** (Figure 5A) and **1m** (Figure 5B) in a concentration-dependent manner. Furthermore, compound **1m**, similar to verapamil, a well-known P-gp inhibitor, enhanced the sensitivity of K562/ADR cells to both ADR and VRN, significantly reducing IC_{50} values (Figure

https://doi.org/10.1021/acsomega.5c00262
ACS Omega 2025, 10, 18720−18732

Table 3. Effects of 1d and 1m on Proliferation of the K562/ADR Multidrug-Resistant Cell[a]

	IC_{50} (nM)		
compounds	K562	K562/ADR	RF
paclitaxel	1.57 ± 1.50	>10,000	>6000
vinorelbine	1.57 ± 1.12	326.45 ± 42.50	230.86
adriamycin	26.70 ± 0.82	2839.50 ± 1057.12	106.35
1d	5291.33 ± 861.23	4909.50 ± 94.05	0.93
1m	4521.33 ± 805.70	3036.50 ± 34.65	0.67

[a]Data were expressed as means ± SD ($n \geq 2$). Note: RF stands for the resistance factor.

5C,D and Table S1). Therefore, these findings indicated that carborane-containing isoflavonoid derivatives **1d** and **1m** effectively inhibited the expression of P-gp and reversed the multidrug resistance to chemotherapeutic drugs in K562/ADR cells.

*Biodistribution Studies of Compounds **1d** and **1m**.* Next, we tested the biodistribution of compounds **1m** and **1d** using two different approaches. Compound **1m** contains a fluorosulfate group on position 7 of its chromone core. A sulfur [^{18}F]fluoride exchange reaction was carried out to prepare the radiolabeled ^{18}F-**1m**.[33,34] PET imaging and biodistribution studies were performed in mice bearing an MDA-MB-231 xenograft at 1 and 3 h after intravenous administration (Figure 6A–C). This study revealed that this compound remained steady from 1 to 3 h in the blood (1.83 ± 0.55% ID/g at 1 h and 2.06 ± 0.57% ID/g at 3 h), indicating a slow clearance of this compound. It had the highest accumulation in the liver at 1 h postinjection (4.57 ± 1.17% ID/g) and increased at 3 h postinjection (8.13 ± 3.09% ID/g), which could be attributed to the high hydrophobicity of carborane. This result suggested a hepatic metabolism and clearance pathway for this compound. The increased uptake in the large intestine (0.53 ± 0.39% ID/g at 1 h and 4.17 ± 1.79% ID/g at 3 h) convinced that compound **1m** underwent hepatic metabolism followed by biliary excretion to the small intestine and eventually accumulated in the large intestine. The PET image also showed a strong radioactive signal in the bladder, suggesting that compound **1m** was also excreted through the urine. We observed that there were signals at elbows and knees in the PET image at 3 h postinjection, as well as the increased uptake in the bone from 1 to 3 h postinjection (0.82 ± 0.32% ID/g at 1 h and 2.86 ± 1.77% ID/g at 3 h). This indicated that the fluorosulfate group was not stable enough *in vivo* and free ^{18}F was dissociated from its parent compound. However, overall, the dissociated ^{18}F signal was minimal and did not affect our analysis.[35,36] The uptake of ^{18}F-**1m** in the tumor is comparable to the uptake in the muscle (0.36 ± 0.29% ID/g at 1 h and 0.42 ± 0.18% ID/g at 3 h). This is not a surprising result since our tested compound was not designed for a specific tumor target. However, this result could help for further effective dosing. The brain uptake of compound ^{18}F-**1m** was 0.17 ± 0.07% ID/g at 1 h and 0.29 ± 0.18% ID/g at 3 h. Although it was lower than the other organs due to the blood–brain barrier, it was higher than compounds such as ^{68}Ga-PSMA11 (0.013 ± 0.004% ID/g at 1 h postinjection).[15] The brain/blood uptake ratio is 0.14 at 3 h postinjection. This indicates partial penetration of compound ^{18}F-**1m** through the blood–brain barrier.

For the other compounds that do not have a ^{18}F labeling position, a boron ICP-mass approach could be applied to measure the biodistribution.[37,38] Compound **1d** was selected as a representative for this biodistribution test. Since the PET imaging study has shown that the uptake at the tumor and

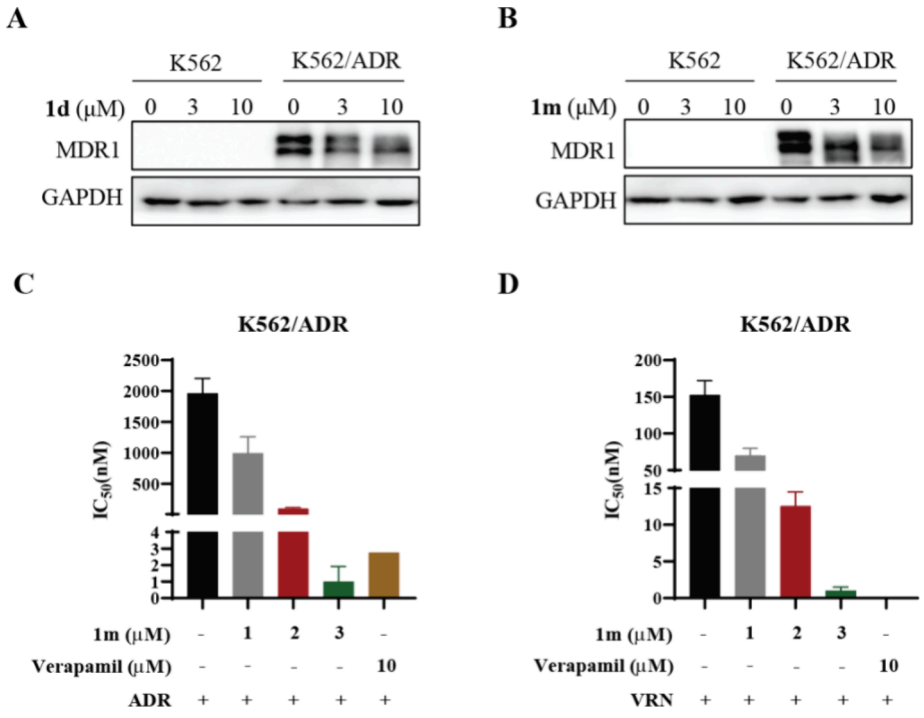

Figure 5. Compounds **1d** and **1m** reverse multidrug resistance in K562/ADR cells. (A, B) Western blot analyses of K562 and K562/ADR after treatment with a concentration gradient of **1d** or **1m** for 48 h. (C, D) IC_{50} values of **1m** and verapamil in reversing the resistance of K562/ADR to ADR or VRN.

https://doi.org/10.1021/acsomega.5c00262
ACS Omega 2025, 10, 18720–18732

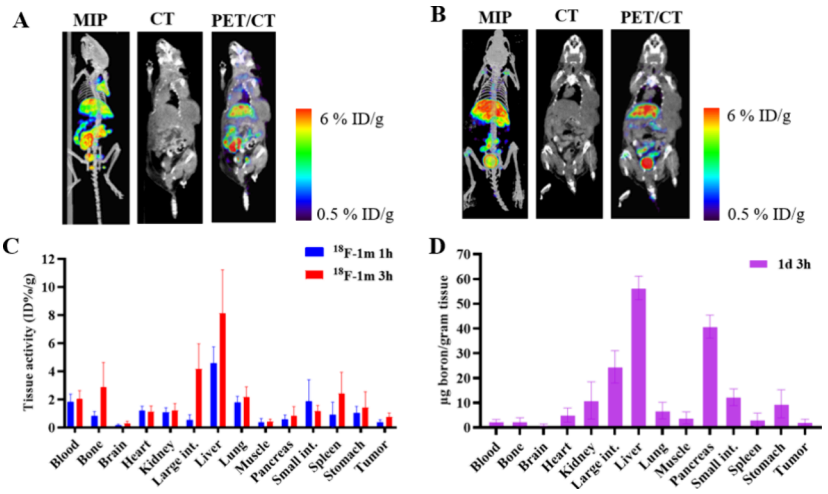

Figure 6. (A) PET imaging results of compound ^{18}F-**1m** at 1 h postinjection. (B) PET imaging results of compound ^{18}F-**1m** at 3 h postinjection. (C) ^{18}F-**1m** biodistribution at 1 and 3 h postinjection. (D) *In vivo* boron biodistribution analysis of compound **1d** at 3 h postinjection.

many other organs at 3 h are higher than that at 1 h postinjection, we chose 3 h postinjection as the best time point for organ collection in this study. The results are shown in Figure 6D. The boron content in the blood was 2.28 ± 0.99 μg/g of tissue. Consistent with the PET study, the liver had the highest boron content (56.37 ± 4.71 μg/g). In contrast, the boron content in the pancreas was surprisingly high, at 40.74 ± 4.67 μg/g of tissue. In our previous BNCT study, we also observed that certain compounds had very high boron uptake in the pancreas.[15] The tumor uptake was 2.18 ± 1.18 μg/g of tissue, similar to the boron level in the blood. The boron content in the brain was 1.03 ± 0.43 μg/g. The brain/blood uptake ratio is 0.45 at 3 h postinjection, indicating a moderate penetration of compound **1d** through the blood−brain barrier.

CONCLUSIONS

In this study, we replaced the phenyl group of isoflavonoids with carborane and prepared a series of novel carborane-containing isoflavonoid analogues. Compounds **1d**, **1g**, and **1m** exhibited significantly improved and broad antiproliferative activities compared to their parent isoflavonoid compounds. The SAR analysis showed that the phenolic hydroxyl group on the 7 position of the carborane-containing isoflavone is a key pharmacophore for its antiproliferative activity. The mechanism study revealed that these compounds could induce G1 cell cycle phase arrest and exhibited antitumor activity through the modulation of the JAK/STAT5, PI3K/AKT, and p38 MAPK pathways. Furthermore, we found that compounds **1d** and **1m** maintained their cytotoxicity toward multidrug-resistant cancer cell lines by inhibiting the expression of p-glycoprotein and reversed the multidrug resistance to chemotherapeutic drugs. The biodistribution studies of compounds **1d** and **1m** demonstrated that these compounds circulated in the blood for at least 3 h with the highest accumulation in the liver. Taken together, these results demonstrated that the incorporation of carborane is an effective strategy for isoflavonoid modification. More natural products and pharmaceuticals are being modified for biological activity screening using this strategy in our lab.

EXPERIMENTAL SECTION

Chemistry. Unless otherwise noted, reagents and solvents were obtained from commercial suppliers and were used without further purification. ^{1}H, ^{13}C and ^{11}B NMR spectra were recorded on a Bruker 500 MHz spectrometer, and chemical shifts were reported in parts per million (ppm) downfield from tetramethylsilane (TMS). Coupling constants (*J* values) were reported in Hertz (Hz). Spin multiplicities are described as s (singlet), br (broad singlet), d (doublet), t (triplet), q (quartet), and m (multiplet). Column chromatography was performed on silica gel (200−300 mesh). All tested compounds were purified to 95% purity as determined by reverse-phase HPLC analysis.

Procedure for the Synthesis of Compounds 1b and 1d. *Step 1: (E)-3-(Dimethylamino)-1-(2-hydroxy-4-methoxyphenyl)prop-2-en-1-one (**3b**).* 1-(2-Hydroxy-4-methoxyphenyl)ethan-1-one (830.8 mg, 5.0 mmol) and *N,N*-dimethylformamide dimethyl acetal (1.3 mL, 10.0 mmol) were dissolved in DMF (15 mL). The reaction mixture was heated at 70 °C for 4 h. After TLC showed that the starting materials were consumed, the reaction was quenched with water. The crude product was precipitated. The mixture was filtered, and the filter cake was washed with water to obtain compound **3b** as a yellow solid (1.1 g, 99% yield). ^{1}H NMR (500 MHz, $CDCl_3$): δ 7.84 (d, J = 11.5 Hz, 1H), 7.60 (d, J = 9.0 Hz, 1H), 6.42 (d, J = 2.5 Hz, 1H), 6.38 (dd, J = 9.0, 2.5 Hz, 1H), 5.68 (d, J = 12.0 Hz, 1H), 3.81 (s, 3H), 3.17 (s, 3H), 2.96 (s, 3H).

*Step 2: 3-Iodo-7-methoxy-4H-chromen-4-one (**4b**).* Compound **3b** (1.1 g, 5.0 mmol) and iodine (2.5 g, 10.0 mmol) were added to MeOH (20 mL). The reaction mixture was heated at 40 °C for 2 h. After TLC showed that the starting materials were consumed, saturated $Na_2S_2O_3$ was added to quench the reaction. The mixture was extracted by EA three times. The combined EA layer was dried over Na_2SO_4, evaporated under reduced pressure, and purified by column chromatography (PE/EA = 5:1) to afford compound **4b** as a light yellow solid (1.3 g, 83% yield). ^{1}H NMR (500 MHz, $CDCl_3$): δ 8.21 (s, 1H), 8.15 (d, J = 9.0 Hz, 1H), 7.01 (dd, J = 9.0, 2.5 Hz, 1H), 6.84 (d, J = 2.5 Hz, 1H), 3.91 (s, 3H).

*Step 3: 7-Methoxy-3-((trimethylsilyl)ethynyl)-4H-chromen-4-one (**5b**).* Compound **4b** (1.3 g, 4.2 mmol) was dissolved in THF (10 mL). $Pd(PPh_3)_2Cl_2$ (147.4 mg, 0.21

https://doi.org/10.1021/acsomega.5c00262
ACS Omega 2025, 10, 18720−18732

mmol), CuI (80 mg, 0.42 mmol), ethynyltrimethylsilane (760 μL, 5.1 mmol), and Et_3N (896 μL, 6.72 mmol) were added at 0 °C. The reaction mixture was stirred at room temperature for 3 h. After TLC showed that the starting materials were consumed, the solvent was removed under reduced pressure. The mixture was purified by column chromatography (PE/EA = 5:1) to afford compound **5b** as a brown solid (924 mg, 83% yield). ^{1}H NMR (500 MHz, $CDCl_3$): δ 8.14 (d, *J* = 9.0 Hz, 1H), 8.10 (s, 1H), 6.98 (dd, *J* = 9.0, 2.5 Hz, 1H), 6.83 (d, *J* = 2.5 Hz, 1H), 3.90 (s, 3H), 0.26 (s, 9H).

*Step 4: 3-Ethynyl-7-methoxy-4H-chromen-4-one (**6b**).* Compound **5b** (924 mg, 3.4 mmol) and (+)-camphor-10-sulfonic acid were added to THF (10 mL). TBAF (1.0 M in THF, 6.8 mmol) was added dropwise. The reaction was stirred at room temperature for 0.5 h. After TLC showed that the starting materials were consumed, water was added to quench the reaction. The mixture was extracted by EA three times. The combined EA layer was dried over Na_2SO_4, evaporated under reduced pressure, and purified by column chromatography (PE/EA = 5:1) to afford compound **6b** as a brown solid (646 mg, 95% yield). ^{1}H NMR (500 MHz, $CDCl_3$): δ 8.16 (d, *J* = 9.0 Hz, 1H), 8.12 (s, 1H), 6.99 (dd, *J* = 9.0, 2.5 Hz, 1H), 6.84 (d, *J* = 2.5 Hz, 1H), 3.91 (s, 3H), 3.27 (s, 1H).

*Step 5: 3-(1,2-Dicarba-closo-dodecarboranyl)-7-methoxy-4H-chromen-4-one (**1b**).* Compound **6b** (646 mg, 3.23 mmol), $B_{10}H_{12}(CH_3CN)_2$ (857 mg, 4.2 mmol), and ionic liquid (Bmim)Cl (110 mg, 0.65 mmol) were added into toluene (10 mL). The reaction was refluxed at 110 °C for 3 h. After TLC showed that the starting materials were consumed, the solvent was removed under reduced pressure. The mixture was purified by column chromatography (PE/EA = 10:1) to afford compound **1b** as a white solid (406 mg, 40% yield). ^{1}H NMR (500 MHz, $CDCl_3$): δ 8.18 (s, 1H), 8.06 (d, *J* = 9.0 Hz, 1H), 7.02 (dd, *J* = 9.0, 2.5 Hz, 1H), 6.84 (d, *J* = 2.0 Hz, 1H), 6.24 (s, 1H), 3.92 (s, 3H), 3.10−1.82 (br, 10H). ^{13}C NMR (126 MHz, $CDCl_3$): δ 174.1, 164.9, 157.2, 156.6, 127.6, 117.4, 117.0, 115.8, 100.0, 69.8, 58.7, 56.1. ^{11}B NMR (162 MHz, $CDCl_3$): δ −3.48, −4.26, −8.79, −10.11, −12.22, −13.45. HRMS (ESI, *m*/*z*) calcd for $C_{12}H_{19}B_{10}O_3$ $[M + H]^+$: 319.2332, found: 319.2327.

*Step 6: 3-(1,2-Dicarba-closo-dodecarboranyl)-7-hydroxy-4H-chromen-4-one (**1d**).* Compound **1b** (406 mg, 1.3 mmol) was dissolved in 1,2-dichloroethane (5 mL), and BBr_3 (2.0 M in DCM, 2.6 mmol) was added dropwise at 0 °C. The reaction was heated to 70 °C and stirred overnight. After TLC showed that the starting materials were consumed, saturated NH_4Cl was added to quench the reaction. The mixture was extracted by EA three times. The combined EA layer was dried over Na_2SO_4, evaporated under reduced pressure, and purified by column chromatography (PE/EA = 5:1) to afford compound **1d** as a white solid (350 mg, 89% yield). ^{1}H NMR (500 MHz, $CDCl_3$): δ 8.20 (s, 1H), 8.05 (d, *J* = 8.5 Hz, 1H), 6.95 (d, *J* = 8.0 Hz, 1H), 6.86 (s, 1H), 6.29 (s, 1H), 6.18 (s, 1H), 3.06−1.61 (br, 10H). ^{13}C NMR (126 MHz, $CDCl_3$): δ 174.4, 161.5, 157.1, 156.9, 128.2, 117.6, 117.0, 116.0, 102.9, 69.7, 58.6. ^{11}B NMR (162 MHz, $CDCl_3$): δ −3.49, −4.27, −8.88, −10.13, −12.23, −13.68. HRMS (ESI, *m*/*z*) calcd for $C_{11}H_{17}B_{10}O_3$ $[M + H]^+$: 305.2176, found: 305.2169.

Procedure for the Synthesis of Compound 1a. *3-Ethynyl-4H-chromen-4-one (**6a**).* Compound **4a** (563 mg, 2.5 mmol) was dissolved in Et_3N (8 mL). $Pd(PPh_3)_2Cl_2$ (88 mg, 0.13 mmol), CuI (4.8 mg, 0.025 mmol), and ethynyltrimethylsilane (745 μL, 5.0 mmol) was added. The reaction was stirred at room temperature for 3 h. After TLC showed that the starting materials were consumed, the solvent was removed under reduced pressure. The mixture was purified by column chromatography (PE/EA = 20:1) to afford compound **5b** as a brown solid (273 mg, 45% yield). The solid was directly dissolved in THF (3 mL), and (+)-camphor-10-sulfonic acid was added. TBAF (1.0 M in THF, 2.2 mmol) was added dropwise. The reaction was stirred at room temperature for 0.5 h. After TLC showed that the starting materials were consumed, water was added to quench the reaction. The mixture was extracted by EA three times. The combined EA layer was dried over Na_2SO_4, evaporated under reduced pressure, and purified by column chromatography (PE/EA = 20:1) to afford compound **6a** as a brown solid (151 mg, 65% yield). ^{1}H NMR (500 MHz, $CDCl_3$): δ 8.27 (dd, *J* = 8.0, 1.0 Hz, 1H), 8.20 (s, 1H), 7.72−7.68 (m, 1H), 7.50−7.41 (m, 2H), 3.28 (s, 1H).

*3-(1,2-Dicarba-closo-dodecarboranyl)-4H-chromen-4-one (**1a**).* Compound **1a** was prepared using a similar method as described for compound **1b**, except for using **6a** as the starting material. Compound **1a** was obtained as a white solid (yield 30%). ^{1}H NMR (500 MHz, $CDCl_3$): δ 8.28 (s, 1H), 8.18 (d, *J* = 8.0 Hz, 1H), 7.75−7.72 (m, 1H), 7.50−7.46 (m, 2H), 6.18 (s, 1H), 3.02−1.71 (br, 10H). ^{13}C NMR (126 MHz, $CDCl_3$): δ 174.8, 157.1, 155.3, 134.7, 126.3, 126.2, 123.7, 118.1, 117.2, 69.7, 58.62. ^{11}B NMR (162 MHz, $CDCl_3$): δ −3.33, −4.11, −8.69, −10.01, −12.06, −13.28. HRMS (ESI, *m*/*z*) calcd for $C_{11}H_{17}B_{10}O_2$ $[M + H]^+$: 289.2227, found: 289.2218.

Procedure for the Synthesis of Compound 1c. *(E)-1-(4-(Benzyloxy)-2-hydroxyphenyl)-3-(dimethylamino)prop-2-en-1-one (**3c**).* Compound **3c** was prepared using a similar method as described for compound **3b**, except for using 1-(4-(benzyloxy)-2-hydroxyphenyl)ethan-1-one as the starting material. Compound **3c** was obtained as a yellow solid (yield 99%). ^{1}H NMR (500 MHz, $CDCl_3$): δ 7.84 (d, *J* = 10.0 Hz, 1H), 7.61 (d, *J* = 8.5 Hz, 1H), 7.43−7.31 (m, 5H), 6.50 (d, *J* = 2.0 Hz, 1H), 6.45 (d, *J* = 8.5 Hz, 1H), 5.68 (d, *J* = 11.0 Hz, 1H), 5.07 (s, 2H), 3.16 (s, 3H), 2.96 (s, 3H).

*7-(Benzyloxy)-3-iodo-4H-chromen-4-one (**4c**).* Compound **4c** was prepared using a similar method as described for compound **4b**, except for using **3c** as the starting material. Compound **4c** was obtained as a slight yellow solid (yield 89%). ^{1}H NMR (500 MHz, $CDCl_3$): δ 8.20 (s, 1H), 8.16 (d, *J* = 9.0 Hz, 1H), 7.45−7.35 (m, 5H), 7.08 (dd, *J* = 9.0, 2.0 Hz, 1H), 6.91 (d, *J* = 2.5 Hz, 1H), 5.16 (s, 2H).

*7-(Benzyloxy)-3-((trimethylsilyl)ethynyl)-4H-chromen-4-one (**5c**).* Compound **5c** was prepared using a similar method as described for compound **5b**, except for using **4c** as the starting material. Compound **5c** was obtained as a brown solid (yield 73%). ^{1}H NMR (500 MHz, $CDCl_3$): δ 8.15 (d, *J* = 8.5 Hz, 1H), 8.09 (s, 1H), 7.42−7.37 (m, 5H), 7.06 (d, *J* = 7.0 Hz, 1H), 6.90 (s, 1H), 5.15 (s, 2H), 0.26 (s, 9H).

*7-(Benzyloxy)-3-ethynyl-4H-chromen-4-one (**6c**).* Compound **6c** was prepared using a similar method as described for compound **6b**, except for using **5c** as the starting material. Compound **6c** was obtained as a brown solid (yield 93%). ^{1}H NMR (500 MHz, $CDCl_3$): δ 8.17 (d, *J* = 9.0 Hz, 1H), 8.11 (s, 1H), 7.45−7.37 (m, 5H), 7.07 (dd, *J* = 9.0, 2.0 Hz, 1H), 6.91 (d, *J* = 2.0 Hz, 1H), 5.16 (s, 2H), 3.26 (s, 1H).

*7-(Benzyloxy)-3-(1,2-dicarba-closo-dodecarboranyl)-4H-chromen-4-one (**1c**).* Compound **1c** was prepared using a similar method as described for compound **1b**, except for using

https://doi.org/10.1021/acsomega.5c00262
ACS Omega 2025, 10, 18720−18732

6c as the starting material. Compound **1c** was obtained as a white solid (yield 45%). ^{1}H NMR (500 MHz, $CDCl_3$): δ 8.17 (s, 1H), 8.07 (d, J = 9.0 Hz, 1H), 7.43−7.42 (m, 5H), 7.09 (d, J = 9.0 Hz, 1H), 6.91 (d, J = 2.5 Hz, 1H), 6.24 (s, 1H), 5.17 (s, 2H), 2.92−1.69 (br, 10H). ^{13}C NMR (126 MHz, $CDCl_3$): δ 174.2, 163.8, 157.1, 156.6, 135.2, 128.9, 128.6, 127.6, 127.5, 117.6, 117.0, 116.3, 101.2, 70.8, 69.8, 58.7. ^{11}B NMR (162 MHz, $CDCl_3$): δ −3.49, −4.33, −8.91, −10.38, −12.22, −13.56. HRMS (ESI, m/z) calcd for $C_{18}H_{23}B_{10}O_3$ $[M + H]^+$: 395.2645, found: 395.2634.

Procedure for the Synthesis of Compounds 1e, 1f, and 1g. *(E)-3-(Dimethylamino)-1-(2-hydroxy-4,6-dimethoxyphenyl)prop-2-en-1-one (**3e**).* Compound **3e** was prepared using a similar method as described for compound **3b**, except for using 1-(2-hydroxy-4,6-dimethoxyphenyl)ethan-1-one as the starting material. Compound **3e** was obtained as a yellow solid (yield 99%). ^{1}H NMR (500 MHz, $CDCl_3$): δ 15.62 (s, 1H), 7.90 (d, J = 12.0 Hz, 1H), 6.24 (d, J = 12.0 Hz, 1H), 6.06 (d, J = 2.0 Hz, 1H), 5.90 (d, J = 1.5 Hz, 1H), 3.83 (s, 3H), 3.78 (s, 3H), 3.13 (s, 3H), 2.92 (s, 3H).

*3-Iodo-5,7-dimethoxy-4H-chromen-4-one (**4e**).* Compound **4e** was prepared using a similar method as described for compound **4b**, except for using compound **3e** as the starting material. Compound **4e** was obtained as a slight yellow solid (yield 42%). ^{1}H NMR (500 MHz, $CDCl_3$): δ 8.08 (s, 1H), 6.43 (d, J = 2.5 Hz, 1H), 6.39 (d, J = 2.5 Hz, 1H), 3.93 (s, 3H), 3.88 (s, 3H).

*5,7-Dimethoxy-3-((trimethylsilyl)ethynyl)-4H-chromen-4-one (**5e**).* Compound **5e** was prepared using a similar method as described for compound **5b**, except for using compound **4e** as the starting material. Compound **5e** was obtained as a brown solid (yield 45%). ^{1}H NMR (500 MHz, $CDCl_3$): δ 7.94 (s, 1H), 6.40 (s, 1H), 6.35 (s, 1H), 3.91 (s, 3H), 3.87 (s, 3H), 0.24 (s, 9H).

*3-Ethynyl-5,7-dimethoxy-4H-chromen-4-one (**6e**).* Compound **6e** was prepared using a similar method as described for compound **6b**, except for using compound **5e** as the starting material. Compound **6e** was obtained as a brown solid (yield 95%). ^{1}H NMR (500 MHz, $CDCl_3$): δ 7.97 (s, 1H), 6.42 (d, J = 2.0 Hz, 1H), 6.37 (d, J = 2.0 Hz, 1H), 3.93 (s, 3H), 3.88 (s, 3H), 3.21 (s, 1H).

*3-(1,2-Dicarba-closo-dodecarboranyl)-5,7-dimethoxy-4H-chromen-4-one (**1e**).* Compound **1e** was prepared using a similar method as described for compound **1b**, except for using compound **6e** as the starting material. Compound **1e** was obtained as a white solid (yield 48%). ^{1}H NMR (500 MHz, $CDCl_3$): δ 8.06 (s, 1H), 6.44 (d, J = 2.5 Hz, 1H), 6.40 (d, J = 2.5 Hz, 1H), 6.30 (s, 1H), 3.94 (s, 3H), 3.89 (s, 3H), 3.01−1.72 (br, 10H). ^{13}C NMR (126 MHz, $CDCl_3$): δ 174.0, 164.9, 161.4, 159.1, 155.0, 117.8, 108.8, 97.1, 92.6, 69.9, 59.0, 56.5, 56.0. ^{11}B NMR (162 MHz, $CDCl_3$): δ −3.62, −4.64, −9.00, −10.21, −12.27, −13.92. HRMS (ESI, m/z) calcd for $C_{13}H_{20}B_{10}O_4$ $[M + H]^+$: 349.2438, found: 349.2437.

*3-(1,2-Dicarba-closo-dodecarboranyl)-5-hydroxy-7-methoxy-4H-chromen-4-one (**1f**).* Compound **1e** (152 mg, 0.4 mmol) was dissolved in 1,2-dichloroethane (2 mL). BBr_3 (2.0 M in DCM, 0.8 mmol) was added dropwise at 0 °C. The reaction mixture was heated to 40 °C and stirred overnight. After TLC showed that the starting materials were consumed, saturated NH_4Cl was added to quench the reaction. The mixture was extracted by EA three times. The combined EA layer was dried over Na_2SO_4, evaporated under reduced pressure, and purified by column chromatography (PE/EA = 8:1) to afford compound **1f** as a white solid (119 mg, 89% yield). ^{1}H NMR (500 MHz, $CDCl_3$): δ 12.10 (s, 1H), 8.12 (s, 1H), 6.40 (d, J = 1.5 Hz, 2H), 6.02 (s, 1H), 3.87 (s, 3H), 3.15−1.76 (br, 10H). ^{13}C NMR (126 MHz, $CDCl_3$): δ 177.8, 165.3, 161.5, 156.1, 156.0, 114.7, 104.3, 98.2, 91.8, 68.0, 57.6, 55.0. ^{11}B NMR (162 MHz, $CDCl_3$): δ −3.28, −4.07, −8.68, −10.13, −12.14, −13.36. HRMS (ESI, m/z) calcd for $C_{12}H_{19}B_{10}O_4$ $[M + H]^+$: 335.2282, found: 335.2277.

*3-(1,2-Dicarba-closo-dodecarboranyl)-5,7-dihydroxy-4H-chromen-4-one (**1g**).* Compound **1e** (152 mg, 0.4 mmol) was dissolved in 1,2-dichloroethane (2 mL). BBr_3 (2.0 M in DCM, 0.8 mmol) was added dropwise at 0 °C. The reaction mixture was heated to 70 °C and stirred overnight. After TLC showed that the starting materials were consumed, saturated NH_4Cl was added to quench the reaction. The mixture was extracted by EA three times. The combined EA layer was dried over Na_2SO_4, evaporated under reduced pressure, and purified by column chromatography (PE/EA = 5:1) to afford compound **1f** as a white solid (119 mg, 75% yield). ^{1}H NMR (500 MHz, $CDCl_3$): δ 12.16 (s, 1H), 8.11 (s, 1H), 6.40 (d, J = 2.0 Hz, 1H), 6.32 (d, J = 2.0 Hz, 1H), 6.27 (s, 1H), 6.01 (s, 1H), 3.08−1.62 (br, 10H). ^{13}C NMR (126 MHz, $CDCl_3$): δ 178.8, 163.3, 162.8, 157.1, 115.7, 105.3, 100.6, 94.4, 69.0, 58.6. ^{11}B NMR (162 MHz, $CDCl_3$): δ −3.29, −4.05, −8.65, −10.06, −12.16, −13.31. HRMS (ESI, m/z) calcd for $C_{11}H_{17}B_{10}O_4$ $[M + H]^+$: 321.2125, found: 321.2115.

Procedure for the Synthesis of Compounds 1h, 1i, 1j, and 1k. *3-(1,2-Dicarba-closo-dodecarboranyl)-7-methoxychroman-4-ol (**1h**).* Compound **1b** (96 mg, 0.3 mmol) was dissolved in THF (1 mL). $NaBH_4$ was added slowly to this mixture at 0 °C. The reaction mixture was stirred at room temperature for 8 h. After TLC showed that the starting materials were consumed, water was added to quench the reaction. The mixture was extracted by EA three times. The combined EA layer was dried over Na_2SO_4, evaporated under reduced pressure, and purified by column chromatography (PE/EA = 5:1) to afford compound **1h** as a white solid (65 mg, 67% yield). ^{1}H NMR (500 MHz, $CDCl_3$): δ 7.08 (d, J = 8.5 Hz, 1H), 6.52 (dd, J = 8.5, 2.5 Hz, 1H), 6.38 (d, J = 2.0 Hz, 1H), 4.87 (s, 1H), 4.59 (s, 1H), 4.37 (dd, J = 11.0, 2.0 Hz, 1H), 4.21−4,17 (m, 1H), 3.77 (s, 3H), 2.83 (d, J = 12.0 Hz, 1H), 2.80−1.76 (br, 10H). ^{13}C NMR (126 MHz, $CDCl_3$): δ 161.8, 154.5, 130.3, 115.3, 108.5, 101.3, 74.0, 65.9, 64.1, 59.7, 55.5, 43.2. ^{11}B NMR (162 MHz, $CDCl_3$): δ −2.70, −3.77, −9.14, −9.63, −12.15, −13.21, −14.16. HRMS (ESI, m/z) calcd for $C_{12}H_{23}B_{10}O_3$ $[M-OH]^+$: 305.2545, found: 305.2530.

*3-(1,2-Dicarba-closo-dodecarboranyl)-7-methoxychroman-4-one (**1i**).* Compound **1h** (65 mg, 0.2 mmol) was dissolved in DCM (1 mL). MnO_2 (44 mg, 0.5 mmol) was added to this mixture. The reaction was stirred at room temperature for 8 h. After TLC showed that the starting materials were consumed, the reaction was filtered to remove MnO_2. The filtration was evaporated under reduced pressure and purified by column chromatography (PE/EA = 5:1) to afford compound **1i** as a white solid (60 mg, 98% yield). ^{1}H NMR (500 MHz, $CDCl_3$): δ 7.85 (d, J = 9.0 Hz, 1H), 6.64 (dd, J = 8.5, 2.0 Hz, 1H), 6.42 (d, J = 2.0 Hz, 1H), 4.65 (dd, J = 12.0, 4.5 Hz, 1H), 4.56 (dd, J = 12.0, 4.5 Hz, 1H), 4.46 (s, 1H), 3.86 (s, 3H), 3.29 (t, J = 4.0 Hz, 1H), 2.97−1.66 (br, 10H). ^{13}C NMR (126 MHz, $CDCl_3$): δ 186.0, 167.2, 163.5, 129.7, 113.6, 111.6, 100.6, 70.8, 70.1, 59.4, 55.8, 48.8. ^{11}B NMR (162 MHz, $CDCl_3$): δ −2.41, −4.04, −9.08, −9.85,

https://doi.org/10.1021/acsomega.5c00262
ACS Omega 2025, 10, 18720−18732

−12.38, −13.65. HRMS (ESI, m/z) calcd for $C_{12}H_{21}B_{10}O_3$ $[M + H]^+$: 321.2489, found: 321.2479.

*3-(1,2-Dicarba-closo-dodecarboranyl)-7-methoxy-2H-chromene (**1j**).* Compound **1h** (65 mg, 0.2 mmol) was dissolved in 1,2-dichloroethane (1 mL). Polyphosphoric acid (100 mg) was added to this mixture. The reaction mixture was refluxed at 80 °C for 8 h. After TLC showed that the starting materials were consumed, water was added to quench the reaction. The mixture was extracted with DCM three times. The combined DCM layer was dried over Na_2SO_4, evaporated under reduced pressure, and purified by column chromatography (PE/EA = 8:1) to afford compound **1j** as a white solid (37 mg, 56% yield). ^{1}H NMR (500 MHz, $CDCl_3$): δ 6.94 (d, J = 8.5 Hz, 1H), 6.63 (s, 1H), 6.47 (dd, J = 8.5, 2.5 Hz, 1H), 6.38 (d, J = 2.0 Hz, 1H), 4.73 (s, 2H), 3.81 (d, J = 9.5 Hz, 1H), 3.78 (s, 3H), 2.84−1.76 (br, 10H). ^{13}C NMR (126 MHz, $CDCl_3$): δ 162.1, 154.6, 128.7, 126.7, 121.5, 113.7, 108.2, 101.4, 74.5, 67.2, 61.2, 55.5. ^{11}B NMR (162 MHz, $CDCl_3$): δ −2.10, −4.09, −9.12, −11.66, −12.21, −13.03. HRMS (ESI, m/z) calcd for $C_{12}H_{21}B_{10}O_2$ $[M + H]^+$: 305.2540, found: 305.2532.

*3-(1,2-Dicarba-closo-dodecarboranyl)-7-methoxychromane (**1k**).* Compound **1j** (37 mg, 0.1 mmol) was dissolved in THF (1 mL). A 5% wet Pd/C (10 mg) was added to this mixture. The reaction was stirred for 6 h under a H_2 atmosphere. After TLC showed that the starting materials were consumed, the mixture was evaporated under reduced pressure and purified by column chromatography (PE/EA = 8:1) to afford compound **1k** as a white solid (35 mg, 98% yield). ^{1}H NMR (500 MHz, $CDCl_3$): δ 6.93 (d, J = 8.5 Hz, 1H), 6.49 (dd, J = 8.5, 2.5 Hz, 1H), 6.36 (d, J = 2.5 Hz, 1H), 4.36−4.33 (m, 1H), 3.83−3.81 (m, 1H), 3.75 (m, 4H), 2.92−2.90 (m, 1H), 2.79−2.76 (m, 2H), 2.75−1.72 (br, 10H). ^{13}C NMR (126 MHz, $CDCl_3$): δ 158.6, 153.1, 129.0, 110.2, 107.3, 100.3, 75.1, 67.8, 58.8, 54.3, 36.9, 30.3. ^{11}B NMR (162 MHz, $CDCl_3$): δ −2.47, −4.19, −9.20, −11.92, −13.35. HRMS (ESI, m/z) calcd for $C_{12}H_{23}B_{10}O_2$ $[M + H]^+$: 307.2696, found: 307.2687.

Procedure for the Synthesis of Compounds 1l and 1m. *3-(1,2-Dicarba-closo-dodecarboranyl)chromane-4,7-diol (**1l**).* Compound **1l** was prepared using a similar method as described for compound **1h**, except for using **1d** as the starting material. Compound **1l** was obtained as a white solid (yield 45%). ^{1}H NMR (500 MHz, $CDCl_3$): δ 7.04 (d, J = 8.5 Hz, 1H), 6.44 (dd, J = 2.5, 8.5 Hz, 1H), 6.32 (d, J = 2.5 Hz, 1H), 5.33 (s, 1H), 4.85 (s, 1H), 4.58 (s, 1H), 4.35−4.35 (m, 1H), 4.20−4.16 (m, 1H), 2.84−2.80 (m, 1H), 2.80−1.79 (br, 10H). ^{13}C NMR (126 MHz, $CDCl_3$): δ 162.6, 157.1, 130.3, 113.3, 112.2, 103.1, 70.8, 69.9, 61.3, 59.5, 48.9. ^{11}B NMR (162 MHz, $CDCl_3$): δ −2.40, −3.93, −9.04, −9.78, −12.25, −13.36. HRMS (ESI, m/z) calcd for $C_{11}H_{20}B_{10}O_3$ $[M-OH]^+$: 291.2388, found: 291.2374.

*3-(1,2-Dicarba-closo-dodecarboranyl)-4-oxo-4H-chromen-7-yl Sulfurofluoridate (**1m**).* Compound **1d** (350 mg, 1.2 mmol) was dissolved in MeCN (5 mL). 1-(Fluorosulfonyl)-2,3-dimethyl-1H-imidazol-3-ium trifluoromethanesulfonate (945 mg, 3.0 mmol) and Et_3N (240 μL, 1.8 mmol) were added to the mixture. The reaction mixture was stirred at room temperature for 1 h. After TLC showed that the starting materials were consumed, the mixture was evaporated under reduced pressure and purified by column chromatography (PE/EA = 15:1) to afford compound **1m** as a white solid (362 mg, 78% yield). ^{1}H NMR (500 MHz, $CDCl_3$): δ 8.33 (d, J = 9.0 Hz, 1H), 8.31 (s, 1H), 7.54 (d, J = 2.0 Hz, 1H), 7.46 (dd, J = 9.0, 2.0 Hz, 1H), 6.06 (s, 1H), 3.02−1.71 (br, 10H). ^{13}C NMR (126 MHz, $CDCl_3$): δ 173.5, 157.6, 155.6, 153.0, 129.4, 123.6, 119.3, 118.2, 111.2, 68.9, 58.5. ^{11}B NMR (162 MHz, $CDCl_3$): δ −3.19, −4.04, −8.68, −10.26, −12.30, −13.52. ^{19}F NMR (471 MHz, $CDCl_3$): δ 39.78. HRMS (ESI, m/z) calcd for $C_{11}H_{16}B_{10}FO_5S$ $[M + H]^+$: 387.1701, found: 387.1689.

Cell Culture. NCI-H1975, NCI-H460, SU-DHL-4, K562, KATO III, MV-4-11, PC-3, MDA-MB-231, A-431, and HPAF-II cell lines were purchased from the American Type Culture Collection (ATCC). DOHH2 and HCT116 cell lines were purchased from Deutsche Sammlung von Mikroorganismen und Zellkulturen (DSMZ). The NUGC-3 cell line was purchased from the Japanese Collection of Research Bioresources (JCRB) Cell Bank. Cells were cultured according to the instructions provided by the manufacturer. The K562/ADR cell line was constructed by gradually increasing the concentration of ADR in the parent K562 cell line. All cell lines were routinely confirmed for Mycoplasma negativity and authenticated using the short tandem repeat (STR) method based on the ATCC, DSMZ, and JCRB database.

Cell Proliferation Assay. Cell proliferation was determined by a sulforhodamine B (SRB) assay for adherent cells or 3-(4,5-dimethyl-2-thiazolyl)-2,5-diphenyl-2H-tetrazolium bromide assay (MTT) for suspended cells.[39] Briefly, cells were seeded in 96-well transparent plates at a density of 4000−6000 cells per well and incubated overnight in a humidified atmosphere with 5% CO_2 at 37 °C. Different concentrations of the test compounds or solvent control were added to triplicate wells. Subsequently, the absorbance (OD) was read at 510 nm for the SRB assay or 570 nm for the MTT assay using a TECAN Spark microplate reader (Spark, TECAN, Switzerland). The potency of compounds in inhibiting cell proliferation was quantified as 50% inhibitory concentration (IC_{50}) values, which were calculated using nonlinear regression analysis with GraphPad Prism 8 software.

Western Blot Analysis. Cells were added into 12-well plates and cultured overnight before being exposed to the test compounds. Following exposure, cells were lysed in a sodium dodecyl sulfate sample buffer. Equal amounts of protein were subjected to sodium dodecyl sulfate polyacrylamide gel electrophoresis (SDS-PAGE) and transferred onto PVDF membranes. Subsequently, the membranes were probed with the primary antibodies followed by incubation with HRP-conjugated secondary antibodies. The proteins were then detected by immunoblotting using an ECL solution (Thermo Fisher Scientific, MA, USA) on a Tanon 4600 imaging system (Tanon, Shanghai, China).

Cell Cycle Analysis by Flow Cytometry. PC-3 and MDA-MB-231 cells were added into 12-well plates and cultured overnight before being exposed to the test compounds. Following exposure, cells were harvested by trypsinization, washed with cold phosphate-buffered saline (PBS), and fixed in 70% ethanol at −20 °C overnight. Then, the cells were washed twice with cold PBS and stained with 50 μg/mL propidium iodide (PI) and 20 μg/mL RNase A at 37 °C for 30 min. The samples were analyzed by flow cytometry (Cytek Aurora 5), with the data acquired from 10,000 cells in general, and analyzed using ModFit 5.0 software (BD Biosciences, Mississauga, Canada).

Radiolabeling of Compound ^{18}F-1m. The [^{18}F]fluoride ion (3.7 GBq) in $H_2{}^{18}O$ was trapped on a QMA cartridge (Sep-Pak Accell Plus QMA Carbonate Plus Light Cartridge,

https://doi.org/10.1021/acsomega.5c00262
ACS Omega 2025, 10, 18720−18732

Waters), which underwent preconditioning with 10 mL of a 0.5 M aqueous $NaHCO_3$ solution followed by 10 mL of water. Subsequently, the adsorbed [^{18}F]fluoride ion was eluted using a solution composed of the phase transfer catalyst K_{222} (Kryptofix 222, 7.5 mg) and K_2CO_3 (1.5 mg), dissolved in a mixed solvent system of MeCN/H_2O (8:2 v/v; total volume, 1 mL). The eluate was then subjected to evaporation at 110 °C for 12 min using a heating block, followed by cooling to 40 °C.[40,41] To this residue was added anhydrous MeCN (1 mL), and the mixture underwent azeotropic drying two more times. The ^{19}F-**1m** solution ((200 μg, 0.52 μmol) in MeCN (1.0 mL)) was added to the reactor. Then, the reaction mixture was heated to 60 °C for 15 min, quenched by 3.0 mL of H_2O, and purified by HPLC (eluent: 20−90% MeCN/H_2O with 0.1% TFA (v/v) in 10 min and maintain 90% MeCN/H_2O for 20 min; 4.0 mL/min; λ = 280 nm) using an Agilent ZORBAX 300SB-C18, 9.4 × 250 mm, 5 μm. The ^{18}F-**1m** from the HPLC column was collected in the bottle and was diluted with 50 mL of H_2O. The solution was transferred to a C18 cartridge (Sep-Pak Plus Short C18 Cartridges, Waters) preconditioned with 10 mL of EtOH and 10 mL of H_2O. The ^{18}F-**1m** was trapped on the C18 cartridge and washed by 10 mL of H_2O. The ^{18}F-**1m** was eluted with 0.2 mL of EtOH and 2 mL of H_2O and transferred to a sterile vial through a 0.22 μm sterile filter. The total activity of ^{18}F-**1m** at the end of the synthesis was 277.5 MBq. The radiochemical purity and identity of ^{18}F-**1m** were confirmed, based on radio-HPLC using a C18, 4.6 × 250 mm, 5 μm analytical column with the HPLC method (eluent: 20−90% MeCN/H_2O with 0.1% TFA (v/v) in 5 min and maintain 90% MeCN/H_2O for 12 min; 1.0 mL/min; λ = 280 nm) (Figure S1).

***In Vivo* PET Imaging and Biodistribution Studies of Compound ^{18}F-1m.** Animal experiments were conducted in compliance with the Institutional Animal Care and Use Committee guidelines of Shanghai Institute of Materia Medica, CAS. Athymic nude mice (female, 6−8 weeks old) were obtained from Beijing HFK Bioscience Co., Ltd. (Beijing, China), raised in air-conditioned rooms with 12 h of light per day, and fed with standard laboratory food and water. For preparing xenograft mice, MDA-MB-231 (5×10^6 cells with Matrigel) was injected subcutaneously in the flank of female athymic nude mice. The xenograft mice were ready for imaging and biodistribution studies when the tumors reached 300−500 mm^3. Mice were anesthetized by isoflurane inhalation followed by injecting 10 μg of compound ^{18}F-**1m** (3.70−5.55 MBq or 100−150 μCi) in saline through the tail vein. The animals were imaged at 1 or 3 h time points postinjection of compound ^{18}F-**1m** with a 20 min acquisition time by using microPET/CT (uBiomicro PET/CT, United Imaging, China). PET imaging data were acquired and reconstructed using a 3D OSEM reconstruction algorithm with an image resolution of 0.6 mm. Imaging data were viewed and processed using open-source Amide software.

For the biodistribution study, the MDA-MB-231 tumor-bearing mice were sacrificed at the 1 or 3 h time points postinjection of compound ^{18}F-**1m**. Blood was collected by a cardiac puncture. Major organs (bone, brain, heart, kidney, large intestine, liver, lung, muscle, pancreas, small intestine, spleen, stomach, and subcutaneous tumor) were harvested, weighed, and counted in an automated gamma counter (Hidex). The percent injected dose per gram of tissue (% ID/g) was calculated by comparison to standards of known radioactivity.

Biodistribution Study of Compound 1d Using ICP-Mass. A 2 mg portion of compound **1d** was administered in a mixture of saline and DMSO through a single intraperitoneal injection. Mice were sacrificed at 3 h postinjection. Blood was collected by cardiac puncture. Major organs (bone, brain, heart, kidney, large intestine, liver, lung, muscle, pancreas, small intestine, spleen, stomach, and subcutaneous tumor) were harvested and weighed. Tissue samples were digested for 2 days at room temperature in 1 mL of a 1:1 mixture of concentrated sulfuric and nitric acids. After vortexing, 100 μL of the digestion solution was taken out and diluted 100-fold in 9.9 mL of DI water followed by filtering through a 0.22 μm membrane. The samples were processed for boron analysis by ICP-OES and ICP-MS.

Statistical Analysis. GraphPad Prism 8 software was used to analyze and plot the experimental data. Data are shown as the mean ± SEM and mean ± SD in *in vivo* and *in vitro* studies, respectively. Statistical analysis was performed by two-tailed Student's *t* test for comparisons between two groups and one-way ANOVA for comparisons involving more than two groups. $P < 0.05$ was considered statistically significant.

■ ASSOCIATED CONTENT

Supporting Information

The Supporting Information is available free of charge at https://pubs.acs.org/doi/10.1021/acsomega.5c00262.

Supplementary biological evaluation data, detailed radiolabeling and biodistribution data, and characterization spectral data for all new compounds (pictures of ^{1}H NMR, ^{13}C NMR, ^{11}B NMR, and HPLC spectra) (PDF)

■ AUTHOR INFORMATION

Corresponding Authors

Rui Zhang − *Department of Nuclear Medicine, Shanghai General Hospital, Shanghai Jiao Tong University School of Medicine, Shanghai 200080, China*; Phone: +86 021 20680809; Email: rui_sjtu@163.com

Chengying Xie − *Lingang Laboratory, Shanghai 200031, China*; Email: xiecy@lglab.ac.cn

Sinan Wang − *School of Biomedical Engineering & State Key Laboratory of Advanced Medical Materials and Devices, ShanghaiTech University, Shanghai 201210, China*; orcid.org/0000-0002-6282-1408; Email: wangsn@shanghaitech.edu.cn

Authors

Yirong Zhang − *School of Biomedical Engineering & State Key Laboratory of Advanced Medical Materials and Devices, ShanghaiTech University, Shanghai 201210, China; School of Pharmacy, East China University of Science and Technology, Shanghai 200237, China*

Chuwei Yu − *Lingang Laboratory, Shanghai 200031, China*

Linyuan Wang − *School of Biomedical Engineering & State Key Laboratory of Advanced Medical Materials and Devices, ShanghaiTech University, Shanghai 201210, China*

Lina Zhou − *School of Life Science and Technology and Shanghai Institute for Advanced Immunochemical Studies, ShanghaiTech University, Shanghai 201210, China*

Chaofan Li − *School of Biomedical Engineering & State Key Laboratory of Advanced Medical Materials and Devices, ShanghaiTech University, Shanghai 201210, China; College*

https://doi.org/10.1021/acsomega.5c00262
ACS Omega 2025, 10, 18720−18732

of Chemical and Pharmaceutical Engineering, Hebei University of Science and Technology, Shijiazhuang 050018, China

Changxian Yuan − *School of Biomedical Engineering & State Key Laboratory of Advanced Medical Materials and Devices, ShanghaiTech University, Shanghai 201210, China*

Nan Sun − *School of Biomedical Engineering & State Key Laboratory of Advanced Medical Materials and Devices, ShanghaiTech University, Shanghai 201210, China*

Guanxiang Hao − *School of Biomedical Engineering & State Key Laboratory of Advanced Medical Materials and Devices, ShanghaiTech University, Shanghai 201210, China*

Chenyang Ma − *School of Biomedical Engineering & State Key Laboratory of Advanced Medical Materials and Devices, ShanghaiTech University, Shanghai 201210, China*

Yuzhe Lin − *School of Biomedical Engineering & State Key Laboratory of Advanced Medical Materials and Devices, ShanghaiTech University, Shanghai 201210, China*

Hongjing Li − *School of Biomedical Engineering & State Key Laboratory of Advanced Medical Materials and Devices, ShanghaiTech University, Shanghai 201210, China*

Jiali Hong − *School of Biomedical Engineering & State Key Laboratory of Advanced Medical Materials and Devices, ShanghaiTech University, Shanghai 201210, China; School of Pharmacy, East China University of Science and Technology, Shanghai 200237, China*

Jinhua Zhao − *Department of Nuclear Medicine, Shanghai General Hospital, Shanghai Jiao Tong University School of Medicine, Shanghai 200080, China;* orcid.org/0000-0002-8867-7985

Kaiyan Lou − *School of Pharmacy, East China University of Science and Technology, Shanghai 200237, China;* orcid.org/0000-0003-1231-8801

Complete contact information is available at: https://pubs.acs.org/10.1021/acsomega.5c00262

Author Contributions

†Y. Zhang and C. Yu made equal contributions to this work.

Notes

The authors declare no competing financial interest.

■ ACKNOWLEDGMENTS

We gratefully acknowledge financial support from Shanghai-Tech University and Shanghai Pujiang Program (22PJ1410900).

■ ABBREVIATIONS USED

P-gp, P-glycoprotein; ICP-mass, inductively coupled plasma-mass spectrometry; PET, positron emission tomography; BNCT, boron neutron capture therapy; SuFEx, sulfur(VI) fluoride exchange; ADR, adriamycin; PTX, paclitaxel; VRN, vinorelbine; MDR, multidrug resistant; ID/g, injected dose per gram tissue

■ REFERENCES

(1) Rodrigues, T.; Reker, D.; Schneider, P.; Schneider, G. Counting on natural products for drug design. *Nat. Chem.* **2016**, *8* (6), 531−541.

(2) Atanasov, A.; Zotchev, S. B.; Dirsch, V. M.; International Natural Product Sciences Taskforce; Supuran, C. T. Natural products in drug discovery: advances and opportunities. *Nat. Rev. Drug Discovery* **2021**, *20* (3), 200−216.

(3) Guo, Z. The modification of natural products for medical use. *Acta Pharm. Sin. B* **2017**, *7* (2), 119−136.

(4) Hong, B.; Luo, T.; Lei, X. Late-stage diversification of natural products. *ACS Cent. Sci.* **2020**, *6* (5), 622−635.

(5) Dixon, R. A.; Pasinetti, G. M. Flavonoids and isoflavonoids: from plant biology to agriculture and neuroscience. *Plant. Physiol.* **2010**, *154* (2), 453−457.

(6) Singh, M.; Kaur, M.; Silakari, O. Flavones: an important scaffold for medicinal chemistry. *Eur. J. Med. Chem.* **2014**, *84*, 206−239.

(7) Miadoková, E. Isoflavonoids - an overview of their biological activities and potential health benefits. *Interdiscip. Toxicol* **2009**, *2* (4), 211−218.

(8) Chahar, M. K.; Sharma, N.; Dobhal, M. P.; Joshi, Y. C. Flavonoids: a versatile source of anticancer drugs. *Pharmacogn. Rev.* **2011**, *5* (9), 1−12.

(9) Rathee, P.; Chaudhary, H.; Rathee, S.; Rathee, D.; Kumar, V.; Kohli, K. Mechanism of action of flavonoids as anti-inflammatory agents: a review. *Inflamm Allergy Drug Targets* **2009**, *8*, 229−35.

(10) Mengheres, G.; Rice, C. R.; Olajide, O. A.; Hemming, K. Synthesis of novel isoflavone/benzo-delta-sultam hybrids as potential anti-inflammatory drugs. *Bioorg. Med. Chem. Lett.* **2021**, *34*, No. 127761.

(11) Hou, S.; Cohen, G. Genistein: therapeutic and preventive effects, mechanisms, and clinical application in digestive tract tumor. *Evid-based Compl. Alt.* **2022**, *2022*, 1−10.

(12) Alshehri, M. M.; Sharifi-Rad, J.; Herrera-Bravo, J.; Jara, E. L.; Salazar, L. A.; Kregiel, D.; Uprety, Y.; Akram, M.; Iqbal, M.; Martorell, M.; Torrens-Mas, M.; Pons, D. G.; Daştan, S. D.; Cruz-Martins, N.; Ozdemir, F. A.; Kumar, M.; Cho, W. C. Therapeutic potential of isoflavones with an emphasis on daidzein. *Oxid. Med. Cell. Longevity* **2021**, *2021* (1), No. 6331630.

(13) Valliant, J. F.; Guenther, K. J.; King, A. S.; Morel, P.; Schaffer, P.; Sogbein, O. O.; Stephenson, K. A. The medicinal chemistry of carboranes. *Coord. Chem. Rev.* **2002**, *232*, 173−230.

(14) Chen, Y.; Du, F.; Tang, L.; Xu, J.; Zhao, Y.; Wu, X.; Li, M.; Shen, J.; Wen, Q.; Cho, C. H.; Xiao, Z. Carboranes as unique pharmacophores in antitumor medicinal chemistry. *Mol. Ther. Oncolytics* **2022**, *24*, 400−416.

(15) Wang, S.; Blaha, C.; Santos, R.; Huynh, T.; Hayes, T. R.; Beckford-Vera, D. R.; Blecha, J. E.; Hong, A. S.; Fogarty, M.; Hope, T. A.; Raleigh, D. R.; Wilson, D. M.; Evans, M. J.; VanBrocklin, H. F.; Ozawa, T.; Flavell, R. R. Synthesis and initial biological evaluation of boron-containing prostate-specific membrane antigen ligands for treatment of prostate cancer using boron neutron capture therapy. *Mol. Pharmaceutics* **2019**, *16* (9), 3831−3841.

(16) Marfavi, A.; Kavianpour, P.; Rendina, L. M. Carboranes in drug discovery, chemical biology and molecular imaging. *Nat. Rev. Chem.* **2022**, *6* (7), 486−504.

(17) Saretz, S.; Basset, G.; Useini, L.; Laube, M.; Pietzsch, J.; Drăca, D.; Maksimović-Ivanić, D.; Trambauer, J.; Steiner, H.; Hey-Hawkins, E. Modulation of γ-secretase activity by a carborane-based flurbiprofen analogue. *Molecules* **2021**, *26* (10), 2843−2860.

(18) Scholz, M.; Bensdorf, K.; Gust, R.; Hey-Hawkins, E. Asborin: The Carbaborane Analogue of Aspirin. *Chem. Med. Chem.* **2009**, *4* (5), 746−748.

(19) Fujii, S.; Goto, T.; Ohta, K.; Hashimoto, Y.; Suzuki, T.; Ohta, S.; Endo, Y. Potent androgen antagonists based on carborane as a hydrophobic core structure. *J. Med. Chem.* **2005**, *48*, 4654−4662.

(20) Scholz, M.; Hey-Hawkins, E. Carbaboranes as pharmacophores: properties, synthesis, and application strategies. *Chem. Rev.* **2011**, *111* (11), 7035−7062.

(21) Kuhnert, R.; Kuhnert, L.; Sarosi, M.; George, S.; Draca, D.; Paskas, S.; Hofmann, B.; Steinhilber, D.; Honscha, W.; Mijatović, S.; Maksimović-Ivanić, D.; Hey-Hawkins, E. Borcalein: a Carborane-Based Analogue of Baicalein with 12-Lipoxygenase-Independent Toxicity. *ChemMedChem* **2022**, *17* (1), No. e202100588.

(22) Cherry, S. R.; Badawi, R. D.; Karp, J. S.; Moses, W. W.; Price, P.; Jones, T. Total-body imaging: transforming the role of positron emission tomography. *Sci. Transl. Med.* **2017**, *9*, No. eaaf6169.

(23) Schwenck, J.; Sonanini, D.; Cotton, J. M.; Rammensee, H. G.; la Fougère, C.; Zender, L.; Pichler, B. J. Advances in PET imaging of cancer. *Nat. Rev. Cancer* **2023**, *23* (7), 474−490.
(24) Rong, J.; Haider, A.; Jeppesen, T. E.; Josephson, L.; Liang, S. H. Radiochemistry for positron emission tomography. *Nat. Commun.* **2023**, *14*, 3257.
(25) McGale, J. P.; Howell, H. J.; Beddok, A.; Tordjman, M.; Sun, R.; Chen, D.; Wu, A. M.; Assi, T.; Ammari, A.; Dercle, L. Integrating artificial intelligence and PET imaging for drug discovery: a paradigm shift in immunotherapy. *Pharmaceuticals* **2024**, *17* (2), 210.
(26) Ghosh, K. K.; Padmanabhan, P.; Yang, C.; Ng, D. C. E.; Palanivel, M.; Mishra, S.; Halldin, C.; Gulyás, B. Positron emission tomographic imaging in drug discovery. *Drug Discovery Today* **2022**, *27* (1), 280−291.
(27) Wongso, H. Natural product-based radiopharmaceuticals: focus on curcumin and its analogs, flavonoids, and marine peptides. *J. Pharm. Anal.* **2022**, *12* (3), 380−393.
(28) Aliya, S.; Alhammadi, M.; Park, U.; Tiwari, J. N.; Lee, J.; Han, Y.; Huh, Y. S. The potential role of formononetin in cancer treatment: An updated review. *Biomed. Pharmacother.* **2023**, *168*, No. 115811.
(29) Tay, K.-C.; Tan, L. T.-H.; Chan, C. K.; Hong, S. L.; Chan, K.-G.; Yap, W. H.; Pusparajah, P.; Lee, L.-H.; Goh, B.-H. Formononetin: A Review of Its Anticancer Potentials and Mechanisms. *Front. Pharmacol.* **2019**, *10*, 820.
(30) Park, S.; Bazer, F. W.; Lim, W.; Song, G. The O-methylated isoflavone, formononetin, inhibits human ovarian cancer cell proliferation by sub G0/G1 cell phase arrest through PI3K/AKT and ERK1/2 inactivation. *J. Cell Biochem.* **2018**, *119* (9), 7377−7387.
(31) Gottesman, M. M.; Pastan, I. Biochemistry of multidrug resistance mediated by the multidrug transporter. *Annu. Rev. Biochem.* **1993**, *62*, 385−427.
(32) Herzog, C. E.; Tsokos, M.; Bates, S. E.; Fojo, A. T. Increased mdr-1/P-glycoprotein expression after treatment of human colon carcinoma cells with P-glycoprotein antagonists. *J. Biol. Chem.* **1993**, *268* (4), 2946−2952.
(33) Zheng, Q.; Xu, H.; Wang, H.; Du, W. H.; Wang, N.; Xiong, H.; Gu, Y.; Noodleman, L.; Sharpless, K. B.; Yang, G.; Wu, P. Sulfur [18F]Fluoride Exchange Click Chemistry Enabled Ultrafast Late-Stage Radiosynthesis. *J. Am. Chem. Soc.* **2021**, *143* (10), 3753−3763.
(34) Liu, Z.; Li, J.; Li, S.; Li, C.; Sharpless, K. B.; Wu, P. SuFEx click chemistry enabled late-stage drug functionalization. *J. Am. Chem. Soc.* **2018**, *140* (8), 2919−2925.
(35) Czernin, J.; Satyamurthy, N.; Schiepers, C. Molecular mechanisms of bone ^{18}F-NaF deposition. *J. Nucl. Med.* **2010**, *51* (12), 1826−1829.
(36) Gonzalez-Galofre, Z. N.; Alcaide-Corral, C. J.; Tavares, A. A. S. Effects of administration route on uptake kinetics of ^{18}F-sodium fluoride positron emission tomography in mice. *Sci. Rep.* **2021**, *11* (1), 5512.
(37) Li, J.; Sun, Q.; Lu, C.; Xiao, H.; Guo, Z.; Duan, D.; Zhang, Z.; Liu, T.; Liu, Z. Boron encapsulated in a liposome can be used for combinational neutron capture therapy. *Nat. Commun.* **2022**, *13* (1), 2143.
(38) Hu, K.; Yang, Z.; Zhang, L.; Xie, L.; Wang, L.; Xu, H.; Josephson, L.; Liang, S. H.; Zhang, M. Boron agents for neutron capture therapy. *Coord. Chem. Rev.* **2020**, *405*, No. 213139.
(39) Wang, Y.; Yao, M.; Li, C.; Yang, K.; Qin, X.; Xu, L.; Shi, S.; Yu, C.; Meng, X.; Xie, C. Targeting ST8SIA6-AS1 counteracts KRAS^{G12C} inhibitor resistance through abolishing the reciprocal activation of PLK1/c-Myc signaling. *Exp. Hematol. Oncol.* **2023**, *12* (1), 105.
(40) Vaidyanathan, G.; Zalutsky, M. R. Synthesis of N-succinimidyl 4-[^{18}F]fluorobenzoate, an agent for labeling proteins and peptides with ^{18}F. *Nat. Protoc.* **2006**, *1* (4), 1655−1661.
(41) Cleeren, F.; Lecina, J.; Bridoux, J.; Devoogdt, N.; Tshibangu, T.; Xavier, C.; Bormans, G. Direct fluorine-18 labeling of heat-sensitive biomolecules for positron emission tomography imaging using the Al^{18}F-RESCA method. *Nat. Protoc.* **2018**, *13* (10), 2330−2347.

https://doi.org/10.1021/acsomega.5c00262
ACS Omega 2025, 10, 18720−18732